Soft Matter

Accepted Manuscript

ROYAL SOCIETY OF CHEMISTRY

www.rsc.org/softmatter

Soft Matter

RSCPublishing

ARTICLE

Energy Release Rate of a Pressurized Crack in Soft Elastic Materials: Effects of Surface Tension and Large Deformation

Tianshu Liu,[a] Rong Long[b] and Chung-Yuen Hui[a]†,

Cite this: DOI: 10.1039/x0xx00000x

Received 00th January 2012,
Accepted 00th January 2012

DOI: 10.1039/x0xx00000x

www.rsc.org/

In this paper we present a theoretical study on how surface tension affects fracture of soft solids. In classical fracture theory, the resistance to fracture is partly attributed to the energy required to create new surfaces. Thus, the energy released to the crack tip must overcome the surface energy in order to propagate a crack. In soft materials, however, surface tension can cause significant deformation and can reduce the energy release rate for crack propagation by resisting the stretch of crack surfaces. We quantify this effect by studying the inflation of a penny-shaped crack in an infinite elastic body with applied pressure. To avoid numerical difficulty caused by singular fields near the crack tip, we derived an expression for the energy release rate which depends on the applied pressure, the surface tension, the inflated crack volume and the deformed crack area. This expression is evaluated using a newly developed finite element method with surface tension elements. Our calculation shows that, when the elasto-capillary number $\omega \equiv \sigma / Ea$ is sufficiently large, where σ is the isotropic surface tension, E is the small strain Young's modulus and a is the initial crack radius, both the energy release rate and the crack opening displacement of an incompressible neo-Hookean solid are significantly reduced by surface tension. For sufficiently high elasto-capillary number, the energy release rate can be negative for applied pressure less than a critical amount, suggesting that surface tension can cause crack healing in soft elastic materials.

1. Introduction

Understanding how surface tension affects the energy release rate of cracks in soft materials is fundamental to many problems related to material processing, such as adhesion and contact mechanics. For example, when an elastic sphere is in adhesive contact to a flat rigid substrate, the contact radius is determined by a balance of surface energy and the energy release rate of the interface crack exterior to the contact zone, as shown by Johnson-Kendall-Roberts (JKR) theory[1]. Recent experimental and theoretical works by Xu et al[2] and Style et al[3] has demonstrated that JKR theory breaks down for very soft elastic substrates. However, these new experimental results are consistent with a theory that accounts for the effect of surface tension on the energy release rate of the interface crack.

The characteristic length scale that describes the deformation of a solid due to its surface tension σ is given by the ratio between the surface tension and its Young's modulus E. For engineering materials such as metals and ceramics, this "elasto-capillary" length is smaller than atomic dimensions. However, in the past decade, new applications such as replica molding and drug delivery drove the synthesis of soft materials such as hydrogels and elastomers with Young's modulus ranging from 10^2 to 10^6 Pa. The elasto-capillary length of these soft materials ranges from tens of nm to hundreds of μm; as a result, the role of surface tension in driving shape change and deformation of solids can be considerable, as demonstrated by recent experiments and simulations[4-10].

For most liquids, surface tension is isotropic and is numerically equal to surface energy. The problem is far more complex for solids since surface stress is not necessary isotropic[11]. In addition, surface stress and surface energy are different physical quantities which need not be numerically equal, even if surface stress is isotropic. In 1975, Gurtin and Murdoch[12] proposed a continuum formulation of surface stress where surface stress can be decomposed into a residual stress component and a surface strain dependent component. For soft material such as elastomer or hydrogel, which is the primary interest of this work, it is reasonable to assume that surface stress is isotropic. As a first-order approximation, in the following we shall assume that the surface tension σ is a material constant independent of surface strain.

There are few studies examining the role of surface stress in fracture since actual measurements of surface stresses are very difficult to make. In 1986, a theoretical analysis of the elastic fracture behavior under the influence of surface stresses was carried out by Thomson et al[13] in which the surface tension was modeled as line forces acting on the crack tip. More relevant to

this present work is the paper by Wu (1999)[14] and Kim et al (2010, 2012) [15, 16]. Wu's paper in 1999 suggested that the stress intensity factor at the crack tip is reduced by surface stresses. However, the numerical solution of Kim et al in 2010[16] showed that for a plane strain crack loaded in Mode I and Mode II, the near tip stress field is bounded, irrespective of the magnitude of the surface stress (as long as it is not exactly zero). In a later paper, Kim et al (2012)[15] reexamined their numerical solution in greater details and showed that the near tip stress field for a Mode I crack has a logarithmic singularity. In both cases their numerical results suggested that the stress intensity factor near the crack tip (or the local stress intensity factor $K_{local} = K_A + K_{ST}$) is exactly zero. In other words, the applied stress intensity factor K_A is cancelled by the negative stress intensity factor K_{ST} due to surface stresses. Since a zero local stress intensity factor implies that local energy release rate is also zero, there seems to be a discrepancy between the results of Wu's [14] and Kim et al's[15, 16]. However, in Wu's analysis [14], a finite tip radius was introduced to remove the negative stress intensity factor induced by surface tension. This finite tip radius approach was also used in later works of Fu et al[17], Wang et al[18] and Wang and Li[19].

The use of a finite tip radius however, is only one way of dealing with the unbounded negative stress intensity factor due to surface tension. A simple way to understand how this occurs is to consider a plane strain Mode I crack lying on the negative x axis, with the crack tip at x = 0. Without loss in generality, we assume surface stress $\sigma_{\alpha\beta}$ to be isotropic, that is, $\tilde{\boldsymbol{\sigma}} = \sigma\delta_{\alpha\beta}$ where σ is the surface tension (force/length). For this case, the Laplace pressure p_L resisting the opening of the crack (see Fig. 1) is directly proportional to the curvature κ which can be written as

$$\kappa = \frac{\mathrm{v}''}{\left[1+\left(\mathrm{v}'\right)^2\right]^{3/2}} \tag{1}$$

where v is the crack opening displacement and a prime denotes differentiation with respect to x. In the analyses of Wu [14] and Kim et al [16], they assumed that v' is small everywhere and the curvature κ is approximated by v''. Due to this approximation, the governing equation describing the crack tip field is linear and the full machinery of analytic function theory can be used to formulate the crack problem.

We can now understand why K_{local} had to be zero in these analyses, that is, the local stress field near the crack tip cannot have an inverse square root singularity. Indeed, assuming K_{local} is positive, the crack opening displacement near the crack tip must have the form:

$$\mathrm{v} \propto K_{\mathrm{local}}\sqrt{-x}, \qquad x<0 \tag{2}$$

Since $\kappa = \mathrm{v}''$,

$$\kappa \propto K_{\mathrm{local}}\left|x\right|^{-3/2}, \qquad x\to 0^- \tag{3}$$

Thus, the Laplace pressure induced by the deformed crack has a non-integrable singularity. It can be shown that such a singular pressure field will induce an infinite negative stress intensity factor at the crack tip, which means that K_{local} goes to negative infinity. This is a contradiction to the original assumption that K_{local} is positive so the only possibility is $K_{local} = 0$, which means either that the stress is bounded or has a weaker singularity. On the other hand, if v' is retained, then

$$\kappa = \frac{\mathrm{v}''}{\left[1+\left(\mathrm{v}'\right)^2\right]^{3/2}} \approx \frac{\mathrm{v}''}{\left(\mathrm{v}'\right)^3}, \qquad x\to 0^- \tag{4}$$

Note that v'' and $\left(\mathrm{v}'\right)^3$ has exactly the same singularity, so that κ is bounded at the crack tip. As a result, it is possible for the local stress intensity factor to be non-zero. Therefore, it is not necessary to introduce a finite tip radius for the undeformed crack if one is willing to deal with a nonlinear boundary condition (i.e., using the full expression for radius of curvature).

The above discussion and analysis illustrates one of the difficulties of using small strain theory to study fracture. The problem arises since the strains and displacement gradient are no longer small near the crack tip, but the linear elasticity theory assumes that these quantities are small and this assumption can result in paradoxes like the one noted above. A more consistent way to approach the fracture problem is to use large deformation theory. We emphasize that our primary objective in this work is to study fracture in soft materials where large deformation cannot be avoided.

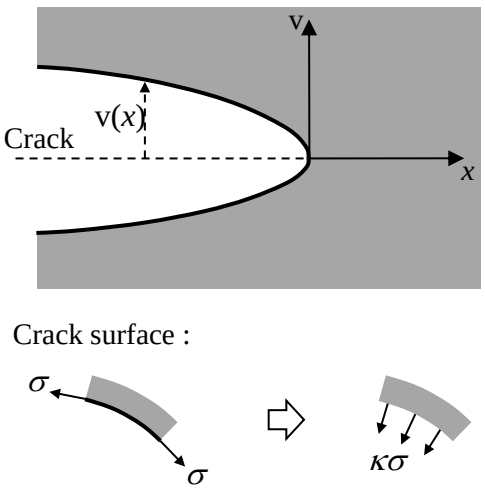

Fig. 1 Surface tension on crack face

The analysis in this work is based on the fully nonlinear equilibrium theory of incompressible hyperelastic solid which allows for arbitrary large deformation. The surface stress is assumed to be isotropic and constant. A newly developed surface tension element[4] is used in conjunction with a commercial finite element code ABAQUS to evaluate the energy release rate. The plan of this paper is as follows. The energy argument for the calculation of energy release rate is established in section 2. Section 3 introduces the mesh and basic procedures used in our finite element calculation. Results are shown in section 4 and section 5 gives an approximated expression for energy release rate. Discussion and summary is given in section 6.

2. Geometry and derivation of Energy Release Rate

Our goal is to determine the energy release rate G of a penny-shaped or circular crack with undeformed radius *a*. The crack lies in the interior of an infinite block of incompressible hyperelastic solid where the strain energy density *W* has the form

$$W = E\Phi(I_1) \tag{5a}$$

where E is the small strain Young's modulus and I_1 is the trace of the Cauchy-Green tensor. The function $\Phi(I_1)$ is assumed to be smooth and obeys[20]

$$\Phi(I_1 \geq 3) \geq 0, \Phi(I_1 = 3) = 0 \tag{5b}$$

The crack is loaded by imposing an internal pressure P on the crack faces. For incompressible solids, this is equivalent to applying a remote hydrostatic tensile stress with magnitude P while keeping the crack surface free of loading except surface tension.

A classical way to calculate G is to use a virtual crack extension method (VCEM). However, this method requires an accurate solution of the stress and strain fields[21]. Due to large deformation, the mesh near the crack tip is highly distorted, so the local stress and deformation fields near the crack tip determined by FEM are much less accurate than global quantities such as the deformed crack volume V. In the following, we derive a simple expression for the energy release rate in terms of P, V and the deformed crack area A. This expression allows us to evaluate G accurately even though the mesh near the crack tip is highly distorted.

The initial configuration is a traction free crack in a stress free solid with no surface tension, and the crack area in this configuration is $A_0 = 2\pi a^2$. It is convenient to "load" the crack in two steps. In the first step, surface tension is increased gradually to its full value σ at zero pressure. At the end of this step, the original flat crack will deform and reduce its area to A_s, with a volume given by V_s. This step is followed by inflating the deformed crack by a hydrostatic pressure P, for example by pushing an incompressible fluid into the crack cavity (see Fig. 2). Let V be the volume of the deformed crack when the applied pressure is P. Since the solid is elastic, the deformation and energy of the system should be independent of loading history and depends only on the final state. In other words, the order of application of surface tension and pressure will not affect our results.

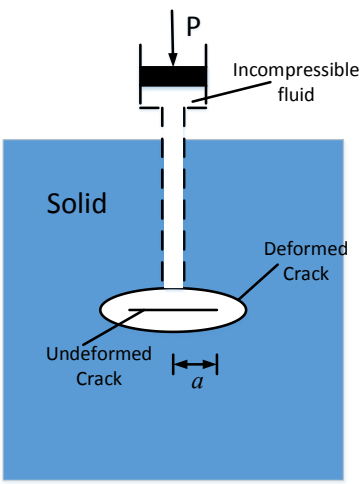

Fig. 2 Schematic of the mechanical loading process.

In the process of turning on the surface tension at zero pressure, the work done by surface tension on the elastic body is

$$-\int_{A_0}^{A_s} \sigma(P=0, A)\, dA \tag{6}$$

Note that the surface tension in this stage is not a constant as it increases from zero to its final value σ. At the end of this step, the potential energy of the surface is σA_s and the elastic energy of the body is given by Eq. (6). Note that since $A_s < A_0$, this energy is positive.

In the second step, the crack is pressurized, the work done by the pressure is

$$\int_{V_s}^{V} P(V^*)\, dV^* \tag{7}$$

This work is used to increase the strain energy of the solid as well as stretching the surface. The potential energy of the pressure load is given by

$$-PV \tag{8}$$

where V is the volume of the crack at the end of the second step. To understand this term, one can imagine that the pressure is applied by a stack of weights. Thus, the system consists of the weights, the elastic solid and its surface. As fluid is forced into the crack, the weight drops and the system lost mechanical potential energy which is given by Eq. (8).

Adding all the energies, the total potential energy of the system PE is:

$$PE = -\int_{A_0}^{A_s} \sigma(P=0, A)\, dA + \int_{V_s}^{V} P\left(V^*\right) dV^* - PV + \sigma A_s \tag{9}$$

After integration by parts, Eq. (9) is simplified as

$$PE = -\int_0^P V\left(P^*\right) dP^* + \int_0^\sigma A\left(P=0, \sigma^*\right) d\sigma^* \tag{10}$$

Dimensional analysis implies that

$$V = a^3 \bar{V}\left(\bar{P}, \omega\right),\ A\left(P=0, \sigma\right) = a^2 \bar{A}\left(\omega\right) \tag{11a}$$

where $\bar{V}$ and $\bar{A}$ are dimensionless functions and

$$\omega = \frac{\sigma}{Ea},\quad \bar{P} = P/E\ , \tag{11b}$$

are the elasto-capillary number and normalized pressure respectively. Substituting Eq. (11a) and Eq. (11b) into Eq. (10) gives:

$$PE = -Ea^3 \left(\int_0^{\bar{P}} \bar{V}\left(\bar{P}^*, \omega\right) d\bar{P}^* - \int_0^{\omega} \bar{A}\left(\omega^*\right) d\omega^* \right) \tag{12}$$

The energy release rate G is, by definition,

$$\begin{aligned} G &= -\frac{1}{2\pi a} \frac{\partial PE}{\partial a}\bigg|_P \\ &= \frac{E}{2\pi a} \frac{\partial}{\partial a} \left[a^3 \int_0^{\bar{P}} \bar{V}\left(\bar{P}^*, \omega\right) d\bar{P}^* - a^3 \int_0^{\omega} \bar{A}\left(\omega^*\right) d\omega^* \right] \\ &= \frac{Ea}{2\pi} \left[3\Psi - \omega \frac{\partial \Psi}{\partial \omega} \right] \end{aligned} \tag{13a}$$

where

$$\Psi\left(\bar{P}, \omega\right) \equiv \int_0^{\bar{P}} \bar{V}\left(\bar{P}^*, \omega\right) d\bar{P}^* - \int_0^{\omega} \bar{A}\left(\omega^*\right) d\omega^* \tag{13b}$$

It is convenient to define a normalized energy release rate Γ by

$$\Gamma \equiv G / Ea = \frac{1}{2\pi}\left[3\Psi - \omega\frac{\partial \Psi}{\partial \omega}\right] \quad (14)$$

If surface tension is neglected, then the normalized energy release rate is a function of pressure only, and reduces to an earlier expression derived by Lin and Hui [22].

3. Finite Element Method

We used a commercial FEM software, ABAQUS, to calculate the displacement field of the crack corresponding to different $\bar{P}$ and elastocapillary number ω. All numerical calculations are carried out by assuming that the elastic solid is incompressible and neo-Hookean, i.e.,

$$W = \frac{E}{6}(I_1 - 3) \quad (15)$$

The built-in hyperelastic function in ABAQUS was used to model the incompressible neo-Hookean material. Symmetry allows us to mesh only the upper half of the elastic solid (see Fig. 3). All lengths are normalized by the undeformed crack radius *a*. The built-in axisymmetric quadrilateral elements (CAX4RH) are used, and on the crack face, a user subroutine (UEL) written in FORTRAN is used to enforce a uniform tension along the crack face. Details about implementation of surface tension element can be found in Xu et al[4]. Eq. (14) is used to evaluate the energy release rate in our FEM. Specifically, in the FEM, the applied pressure and surface tension are changed incrementally from zero. At each step, the deformed crack volume and deformed crack faces area are obtained from the computed crack opening displacement. Using Eq. (13b), Ψ can be calculated by numerical integration and Γ is evaluated using numerical differentiation. Unlike stress fields, the total crack volume *V* and the crack face area *A* are relatively insensitive to the distortion of elements near the crack tip, hence the energy release rate calculated using Eq. (14) is expected to be much more accurate than VCEM. When the elements are too distorted, a re-mesh program is used to ensure convergence and accuracy. A typical mesh used in our simulation is shown in Fig. 4.

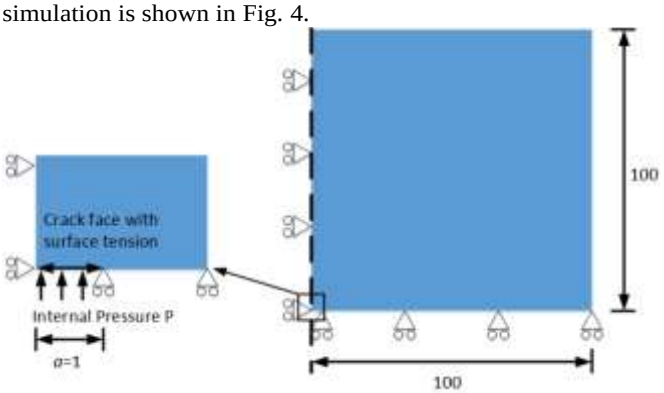

Fig. 3: The geometry and boundary conditions used in our finite element calculation. All lengths are normalized by initial crack radius *a*. The right and upper boundaries are traction free. Symmetry boundary conditions are applied on the left and lower boundaries. Internal pressure and surface tension are applied on crack faces.

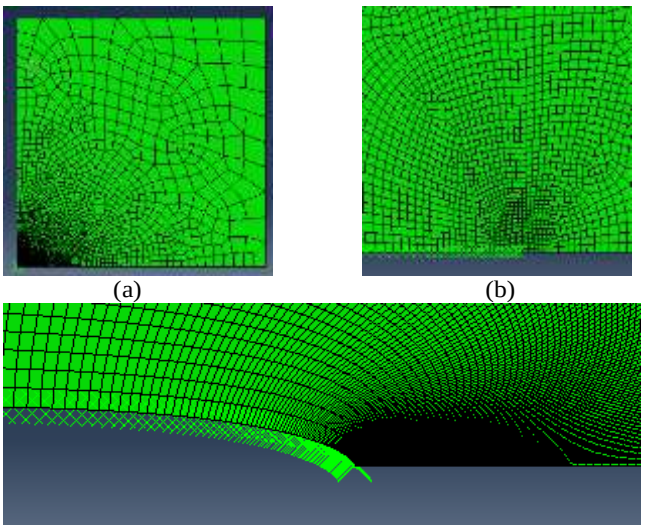

Fig. 4 Mesh used in our FEM calculation: (a) mesh of the full model. (b) zoom-in view of the original coarse mesh near the crack tip. (c) Re-mesh on deformed configuration.

4. Results

The elasto-capillary number is the only material parameter that controls our solution. We give an order of estimate for the elasto-capillary number ω for a soft material with a small crack. If the crack radius is 1mm and the surface tension is 0.1J/m^2, then $\omega = 10^2 (J/m^3)/E$. For a very soft gel with modulus on the order of tens of pascals, ω is of order unity. For rubbers, where the modulus is on the order of $10^6 Pa$, $\omega \approx 10^{-4}$. Fig. 5 (a) plots the normalized crack volume $\bar{V}(\bar{p}, \omega)$ versus the elasto-capillary number ω for three different values of applied pressure. It shows that for soft materials, the reduction of crack volume due to surface tension can be significant.

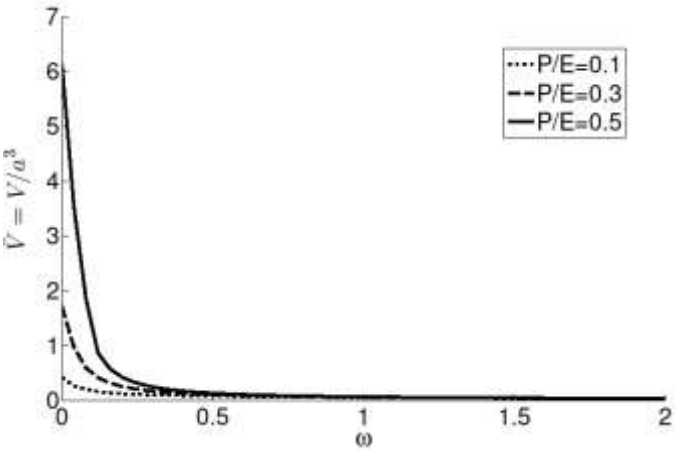

(a)

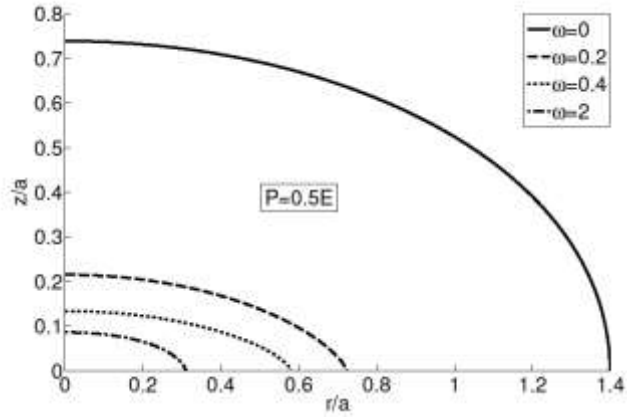

(b)

Fig. 5 (a) Normalized crack volume versus elasto-capillary number ω for different pressures. (b) Crack opening displacements for different elasto-capillary numbers when $p = 0.5E$

Fig.5(b) shows the crack opening profile for different elasto-capillary number when the applied pressure is $0.5E$. Note that as ω increases, the crack shrinks both in the horizontal and vertical directions. The results shown above are for reasonably large pressures. For low pressures, for example, $P = 0.02E$, the results are shown in Fig. 6(a,b). For the case of no surface tension, $\omega = 0$ (point A), the crack is opened by the pressure. As ω is increased from A to B, the crack shrinks in both directions as shown in Fig.6 (b). In this regime, the inward Laplace pressure caused by the surface tension resist crack opening. From B to C, the crack continues to shrink in horizontal direction but opens more in the middle. After the crack volume reaches its maximum at C, the crack opening displacement continues to increase until ω reaches ω_D. After D, the crack starts to shrink in both directions again and eventually the crack volume approaches zero as ω increases. Thus, for a fixed pressure, our results suggest that the crack volume will go to zero in the limit of infinite surface tension or $\omega \to \infty$.

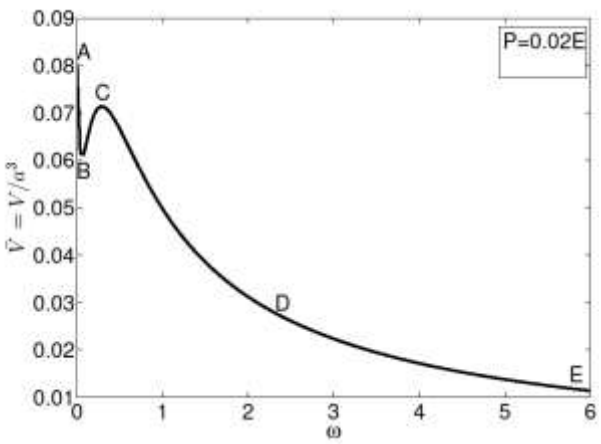

(a)

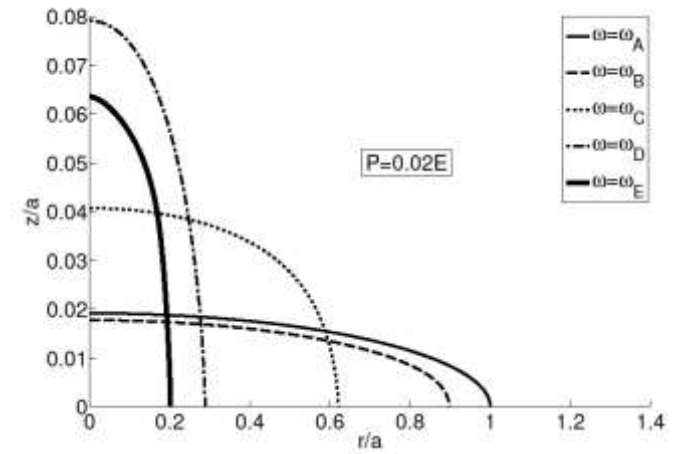

(b)

Fig.6 (a) Normalized crack volume versus elasto-capillary number ω for $P = 0.02E$. (b) Crack opening displacements for different elasto-capillary numbers when $P = 0.02E$

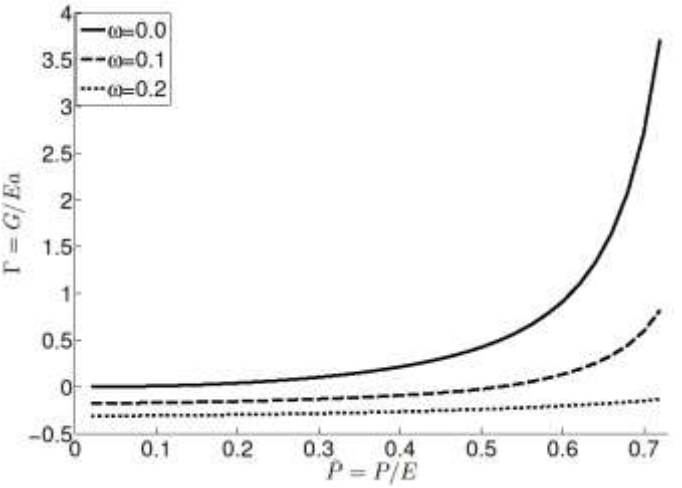

Fig. 7 Change of normalized energy release rate with respect to normalized pressure for different elasto-capillary number

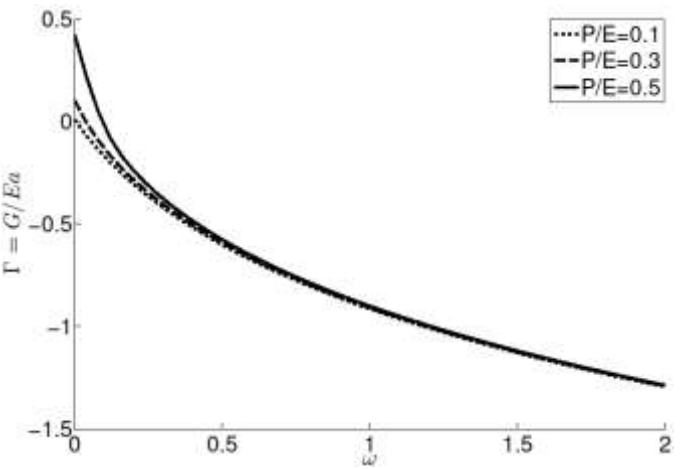

Fig. 8 Change of normalized energy release rate with respect to elasto-capillary number for different normalized pressure

Fig. 7 plots the normalized energy release rate versus normalized pressure for three different elasto-capillary numbers. For zero surface tension, the energy release rate is always positive and increases with pressure. This result is identical to the previous work of Lin and Hui[22]. For $\omega = 0.1$ and $\omega = 0.2$, the energy release rate is negative when pressure is below some critical value. Physically, this means that the crack will have a tendency to heal since the potential energy of the system will decrease when the crack heals.

The dependence of Γ on ω for fixed normalized pressures is shown in Fig. 8. This result suggests that, for any fixed applied pressure, the energy release rate is a monotonic decreasing function of ω so that in the liquid limit, the crack will be closed under a constant pressure load. One may imagine that in the liquid limit, the crack would deform into a sphere with a finite radius, but a straight forward analysis of the potential energy of spherical solution in this limit shows that this solution is unstable under pressure control and thus the sphere will collapse.

5. Approximation for energy release rate

In this section, we give an approximate linearized formula for energy release rate in the limit of very small $\omega = \sigma / Ea$.

Let $\Gamma_0 \equiv \Gamma\left(\bar{P}, \omega = 0\right)$ denote the normalized energy release rate for the case with no surface tension. As shown in Fig. 9, the Γ_0 versus $\bar{P}$ curve of our FEM result can be fitted very well by the expression:

$$\Gamma_0 = \frac{3}{\pi}\bar{P}^2 exp\left[\frac{-1.333\bar{P}^3 + 1.021\bar{P}^2 + 0.0747\bar{P}}{0.72 - \bar{P}}\right] \qquad (16)$$

Note Eq. (16) agrees with the energy release rate in the small strain limit, where

$$\Gamma_0 = \pi\bar{P}^2 / 3, \qquad \bar{P} << 1 \qquad (17)$$

In the previous work of Lin and Hui[22], it was found numerically that the energy release rate tends to diverge at a finite value of $\bar{P} \approx 0.72$. This feature is also included in Eq. (16). However, it must be noted that this divergence is restricted to neo-Hookean solid which underestimates the amount of strain hardening effect. Lin and Hui[22] has shown that the energy release rate does not diverge for materials that exhibit high strain hardening.

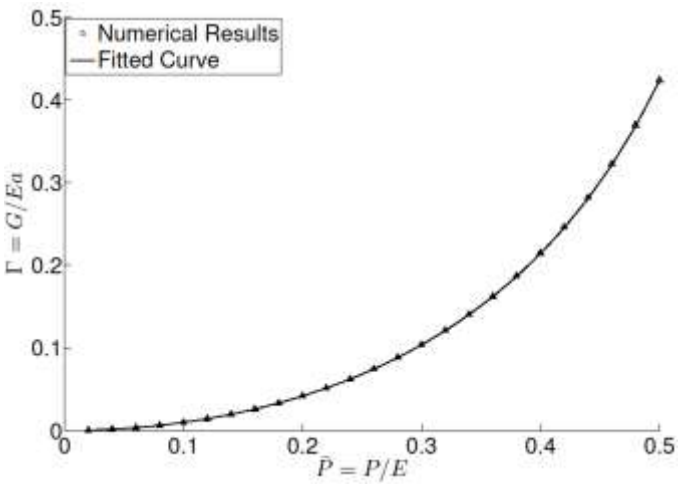

Fig. 9 Normalized energy release rate versus normalized pressure $\bar{P}$, when $\omega = 0$.

The numerical result in Fig. 8 suggests that the normalized energy release rate can be approximated by a linear function of ω when ω is sufficiently small, that is,

$$\Gamma = \Gamma_0 + s(\bar{P})\omega, \qquad \omega << 1 \qquad (18)$$

where s is the slope of the $\Gamma - \omega$ curve when $\omega \to 0$, which depends on the normalized pressure $\bar{P}$. The region of validity of Eq. (18) depends on the normalized pressure, as can be seen in Fig. 8. The dependence of s on $\bar{P}$ is shown in Fig. 10.

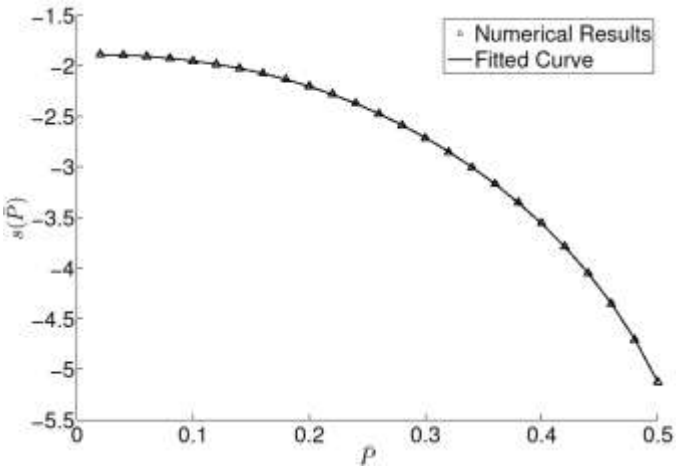

Fig. 10 $s\left(\bar{P}\right) = \partial\Gamma / \partial\omega|_{\omega=0}$ versus normalized pressure $\bar{P}$.

A fit for the s versus $\bar{P}$ curve is

$$s(\bar{P}) = -1.885 - 5.123\bar{P}^2 \exp\left[\frac{4.109\bar{P}^3 - 5.328\bar{P}^2 + 2.045\bar{P}}{0.72 - \bar{P}}\right] \qquad (19)$$

Eq. (19), combined with the Eq. (16), allow us to find an approximate expression for the energy release rate in the limit of small $\omega = \sigma / Ea$, that is,

$$\Gamma = \frac{3}{\pi}\bar{P}^2 exp\left[\frac{-1.333\bar{P}^3 + 1.021\bar{P}^2 + 0.0747\bar{P}}{0.72 - \bar{P}}\right] - \left[1.885 + 5.123\bar{P}^2 \exp\left(\frac{4.109\bar{P}^3 - 5.328\bar{P}^2 + 2.045\bar{P}}{0.72 - \bar{P}}\right)\right]\omega \qquad (20)$$

which provides a good fit to our numerical results in Fig. 8 in the small ω limit.

6. Summary and Discussion

The effect of surface tension on the energy release rate of a penny-shaped crack under internal pressure is determined by the dimensionless elasto-capillary number $\omega = \sigma / Ea$. A simple expression of the energy release rate which involves only the deformed crack volume, deformed crack area, elasto-capillary number and the applied pressure is derived. For a neo-Hookean solid, our finite element results show that the energy release rate is significantly reduced due to surface tension. For pressure lower than a critical value which depends on the elasto-

capillary number, the energy release rate is negative which means the crack has a tendency to heal. This is a nonlinear phenomenon that cannot be captured by the linearized theory. For small ω, an approximated linear function to evaluate the normalized energy release rate Γ is given by

$$\Gamma = \Gamma_0(P/E) + s(P/E)\omega \ , \qquad (21)$$

where Γ_0 is the energy release rate without surface tension and is given by Eq. (16), and S is a dimensionless function that depends on the normalized applied pressure.

Surface energy also plays an important role in fracture energy. For ideally brittle elastic solids, the fracture energy or fracture toughness is twice the surface energy. However, this is rarely the case for most materials because of additional dissipation mechanism. For materials relevant to this work, such as elastomers, the fracture energy is found to be much greater than surface energy, which can be estimated by taking the energy required to break a carbon-carbon bond and multiplying it by the number of bonds crossing a unit area of the fracture plane[24]. Lake and Thomas [24] suggested that most of the energy stored in the chains up to the point of bond rupture is dissipated, so fracture energy in elastomers is amplified by the number of bonds per chain. In this paper, we show that for soft materials, although surface energy is not the dominant factor in setting the fracture energy, surface tension can significantly affect the material deformation and stress field and thus reduces the energy release rate. This is a new and interesting way in which surfaces resist fracture.

Finally, our work assumes that the surface tension is positive but it can be negative[11]. We did not investigate this possibility since a compressive surface stress may cause a buckling instability of the crack faces, which will lead to complications in our numerical method. Whether a negative surface tension will increase the energy release rate is an interesting question subjected to further investigation.

Acknowledgements

C.Y. Hui and Tianshu Liu acknowledge the support of the U.S. Department of Energy, Office of Basic Energy Sciences, Division of Materials Sciences and Engineering under Award DE-FG02-07ER46463. Dr. R. Long helps with the theory as well as with the finite element analysis and writing of the paper and is supported by the Natural Sciences and Engineering Research Council of Canada. The authors thank an anonymous reviewer for his/her helpful comments.

Notes and references

[a] Field of Theoretical and Applied Mechanics, Cornell University, Ithaca, NY 14853.

[b] Department of Mechanical Engineering, University of Alberta, Edmonton, AB T6G 2G8, Canada.

† Corresponding Author, email: ch45@cornell.edu.

Electronic Supplementary Information (ESI) available: [details of any supplementary information available should be included here]. See DOI: 10.1039/b000000x/

1. K. L. Johnson, K. Kendall and A. D. Roberts, *Proceedings of the Royal Society A: Mathematical, Physical and Engineering Sciences*, 1971, **324**, 301-313.
2. X. Xu, A. Jagota and C.-Y. Hui, *Soft Matter*, 2014.
3. R. W. Style, C. Hyland, R. Boltyanskiy, J. S. Wettlaufer and E. R. Dufresne, *Nature communications*, 2013, **4**, 2728.
4. X. Xu, A. Jagota, S. Peng, D. Luo, M. Wu and C. Y. Hui, *Langmuir : the ACS journal of surfaces and colloids*, 2013, **29**, 8665-8674.
5. S. Mora, C. Maurini, T. Phou, J.-M. Fromental, B. Audoly and Y. Pomeau, *Physical Review Letters*, 2013, **111**.
6. A. Marchand, S. Das, J. H. Snoeijer and B. Andreotti, *Physical Review Letters*, 2012, **108**.
7. R. Style, R. Boltyanskiy, Y. Che, J. Wettlaufer, L. A. Wilen and E. Dufresne, *Physical Review Letters*, 2013, **110**.
8. R. W. Style and E. R. Dufresne, *Soft Matter*, 2012, **8**, 7177.
9. A. Jagota, D. Paretkar and A. Ghatak, *Physical Review E*, 2012, **85**.
10. B. Roman and J. Bico, *Journal of physics. Condensed matter : an Institute of Physics journal*, 2010, **22**, 493101.
11. R. C. Cammarata and K. Sieradzki, *Annual Review of Materials Science*, 1994, **24**, 215-234.
12. M. Gurtin and A. Ian Murdoch, *Archive for Rational Mechanics and Analysis*, 1975, **57**.
13. R. Thomson, T. J. Chuang and I. H. Lin, *Acta Metallurgica*, 1986, **34**, 1133-1143.
14. C. Wu, *Journal of the Mechanics and Physics of Solids*, 1999, **47**, 2469-2492.
15. C. Kim, C. Q. Ru and P. Schiavone, *Mathematics and Mechanics of Solids*, 2012, **18**, 59-66.
16. C. I. Kim, P. Schiavone and C. Q. Ru, *Journal of Elasticity*, 2010, **104**, 397-420.
17. X. L. Fu, G. F. Wang and X. Q. Feng, *International Journal of Fracture*, 2008, **151**, 95-106.
18. G.-F. Wang, X.-Q. Feng, T.-J. Wang and W. Gao, *Journal of Applied Mechanics*, 2008, **75**, 011001.
19. G. F. Wang and Y. Li, *Engineering Fracture Mechanics*, 2013, **109**, 290-301.
20. A. J. M. Spencer, *Continuum Mechanics*, Longman, 1980.
21. D. M. Parks, *Computer Methods in Applied Mechanics and Engineering*, 1977, **12**, 353-364.
22. Y. Y. Lin and C. Y. Hui, *International Journal of Fracture*, 2004, **126**, 205-221.
23. R. Long and C.-Y. Hui, *Soft Matter*, 2010, **6**, 1238.
24. G. J. Lake and A. G. Thomas, *Proceedings of the Royal Society A: Mathematical, Physical and Engineering Sciences*, 1967, **300**, 108-119.